Materials Transactions, Vol. 65, No. 2 (2024) pp. 194 to 198

Quantifying Laser Absorptivity of Ti–6Al–4V Powder through Additive Manufacturing Systems

Hiroshi Honda* and Makoto Watanabe

Research Center for Structural Materials, National Institute for Materials Science, Tsukuba, Ibaraki 305-0047, Japan

In laser metal-based powder-bed fusion additive manufacturing, it is important to know the laser absorptivity of metal powder to elucidate or optimize the manufacturing process and numerical simulation. Laser absorptivity depends on the manufacturing process conditions and the circumstances of the additive manufacturing machine. Therefore, we tried to develop a simple method of measuring laser absorptivity under the same circumstances present in the manufacturing process by using a commercially available additive manufacturing machine.
[doi:10.2320/matertrans.MT-M2023156]

(Received September 28, 2023; Accepted October 31, 2023; Published January 25, 2024)

Keywords: *additive manufacturing, power-bed fusion, Ti–6Al–4V powder, laser absorptivity*

1. Introduction

In laser powder-bed fusion additive manufacturing, powder's absorption of laser energy represents an initial phenomenon with far-reaching effects on subsequent processes and the properties of the resulting product. Therefore, the ability to measure laser absorptivity is necessary for the elucidation or optimization of the manufacturing processes. This ability is also indispensable for numerical simulations of additive manufacturing.

However, the number of materials with known absorptivity is not high, and the light wavelengths of absorptivity are limited. Furthermore, absorptivity is generally measured for ideal flat surfaces. The materials used in laser power-bed fusion additive manufacturing are spherical, and the surface conditions are usually not ideal. Therefore, laser absorptivity is thought to change depending on the surface conditions of the powder used. The temperature dependence of laser absorptivity is also important in order to understand the manufacturing process. However, there are only a few materials for which the temperature dependence of laser absorptivity is known.

One method of measuring light absorptivity involves the use of an integrating sphere. Brandau *et al.*[1] measured absorptivity across a wide range of light wavelengths for various metal powders. However, the measurement circumstances differed from those of additive manufacturing, and the temperature dependence of absorptivity was not measured.

Calorimetric methods have also been used to measure laser absorptivity. Wieting *et al.*[2] measured the laser absorptivity of stainless steel sheets for a CO_2 laser by analyzing the heating rate during laser irradiation, followed by the cooling rate post-irradiation, within a vacuum furnace. They also investigated the temperature dependence of laser absorptivity by varying the furnace temperature. Haag *et al.*[3] measured the laser absorptivity of powder when exposed to a CO_2 laser by considering factors such as laser irradiation time, temperature elevation of the irradiated sample, and subsequent cooling rate. These measurements were conducted in different atmospheres—air, argon, and helium—using specialized equipment designed for this purpose. However, they did not measure the temperature dependence of the laser absorptivity. Rubenchik *et al.*[4,5] investigated the temperature-dependent laser absorptivity of both plate and powder forms of various materials. They employed a dedicated measurement system that utilized a laser diode, eliminating the need for a furnace setup. However, the laser wavelength and the measurement circumstances in the measurement system may differ from those in the additive manufacturing machine to be used. In such cases, it is necessary to consider such differences in order to understand the manufacturing process.

Trapp *et al.*[6] made a dedicated device that imitated laser powder-bed fusion additive manufacturing, and used it to measure laser absorptivity based on the temperature evolution of the specimen. The conditions closely mimicked additive manufacturing conditions, encompassing scenarios that lead to the formation of keyholes. However, the measured laser absorptivity encompasses the entire spectrum of phenomena occurring during the additive manufacturing process, and the precise temperature dependence of laser absorptivity remains uncertain. Moreover, the laser and the measurement circumstances of the dedicated equipment may differ from those of the additive manufacturing machine to be used.

In real situations, the laser, the powder, and the manufacturing circumstance change depending on the additive manufacturing machine and the manufacturing process. The laser absorptivity will also change, and it is necessary to know the laser absorptivity in each situation in order to realize the desired product. Therefore, we tried to measure the laser absorptivity of metal powder by using a commercially available additive manufacturing machine under the same circumstances present in the manufacturing process.

2. Experimental Procedure

Laser absorptivity in this experiment was measured by a calorimetric method similar to that employed by Rubenchik *et al.*[4,5] In the method we used, the temperature of a

*Corresponding author, E-mail: HONDA.Hiroshi@nims.go.jp

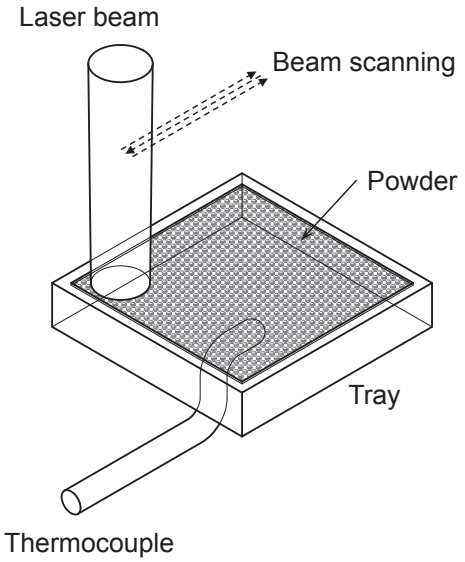

Fig. 1 Schematic of the experimental setup.

specimen during laser irradiation was measured and the laser absorptivity was calculated from energy conservation during the temperature variation. The laser irradiation conditions were chosen such that they could be used by a commercially available additive manufacturing machine.

In the method used by Rubenchik *et al.*,[5] the powder on a tray was irradiated uniformly and continuously by a laser light. In our method, the laser light scans the powder area repeatedly as shown in Fig. 1, under the same circumstances of the manufacturing process that would be used for an additive manufacturing machine. The laser absorptivity was calculated by using the energy conservation in each laser light scan of the powder area.

The laser absorptivity can be calculated by eq. (1), which represents the power conservation:

$$A(T)P = (m_1c_1(T) + m_2c_2(T))\frac{dT}{dt} + L(T). \quad (1)$$

Here, P is laser power, T is temperature, and $A(T)$ is laser absorptivity at temperature T. m_1 and m_2 are the masses of the powder and tray, respectively. $c_1(T)$ and $c_2(T)$ are the specific heats of the powder and tray, respectively. t is time and $L(T)$ is the thermal loss to the surroundings.

The thermal loss depends on the measurement environment of the additive manufacturing machine. When the laser power is zero, namely $P = 0$, eq. (1) becomes as follows:

$$L(T) = -(m_1c_1(T) + m_2c_2(T))\frac{dT}{dt}. \quad (2)$$

The thermal loss in the measurement environment can be evaluated from the specific heats and cooling rate at temperature T. In this experiment, the thermal loss was estimated from the temperature history of the cooling process after the laser heating under the same circumstances as in the heating process.

Equation (1) can be differentiated by using the time interval of laser scanning of the powder area Δt and solved for $A(T)$ as follows:

$$A(T) = \frac{(m_1c_1(T) + m_2c_2(T))\Delta T + L(T)\Delta t}{E}. \quad (3)$$

Here, E and ΔT are the irradiated energy and the temperature rise during the time interval Δt, respectively. The laser absorptivity in this experiment was calculated by eq. (3).

The laser powder-bed fusion additive manufacturing machine used in this experiment was the SLM Solutions SLM280. The laser wavelength was 1070 nm. The process chamber was filled with argon gas. The specimen as shown in Fig. 1 was set in the process chamber, whose environment was the same as that of the manufacturing process of the machine.

The material of the metal tray and powder was titanium alloy Ti–6Al–4V. The tray size was 10 mm × 10 mm × 1 mm. The top surface of the tray had a machined recessed flat portion with 0.10 mm depth. The metal powder was evenly placed on the recessed portion to the height of the rim. A commercially available powder, CONCEPT LASER CL 41TI ELI, was used. The mass of the tray was 0.4083 g, and the mass of the tray with the powder was 0.4242 g. The temperature was measured by using a thermocouple attached to the center of the bottom surface of the tray.

The laser beam was Gaussian and scanned the powder area in a meander hatch pattern as shown in Fig. 1. The scanning process was replicated 10 times, with 1 s intervals between scans. The incident angle of the laser beam on the specimen was almost normal, as shown in Fig. 1. To avoid the melting of the metal powder, the spot size of the laser beam on the specimen was expanded and the scan speed was set to high. The spot size and scan speed were estimated to be about 2.2 mm and 16 m/s, respectively. There were 161 hatch lines in the powder area. The laser power was changed in the order of 50 W, 60 W, and 70 W without exchanging the metal powder in this experiment.

Moreover, the laser absorptivity of a machined flat surface of the titanium alloy Ti–6Al–4V was measured by irradiating the metal tray without the metal powder under the same experimental conditions.

For the calculation of laser absorptivity in eq. (3), the temperature-dependent specific heat was incorporated, utilizing a fitting formula derived from experimental data for the titanium alloy Ti–6Al–4V.[7]

3. Results and Discussion

Figure 2 illustrates the recorded temperature history of the specimen. It was measured for the tray without powder at 70 W laser power. The temperature history shows a steplike pattern aligned with the 1 s time interval between scans.

For the calculation of laser absorptivity using the values of ΔT and Δt in eq. (3), the differences between the local maximums of adjacent steps were employed, as depicted in the inset of Fig. 2. The differences between the local minimums of adjacent steps were also utilized. As seen from the temperature history magnified in the inset in Fig. 2, the cooling curve gradient changed largely around 10.5 s following the peak temperature in this experiment.

To investigate the change in the cooling curve gradient, a simplified numerical simulation was performed by using an

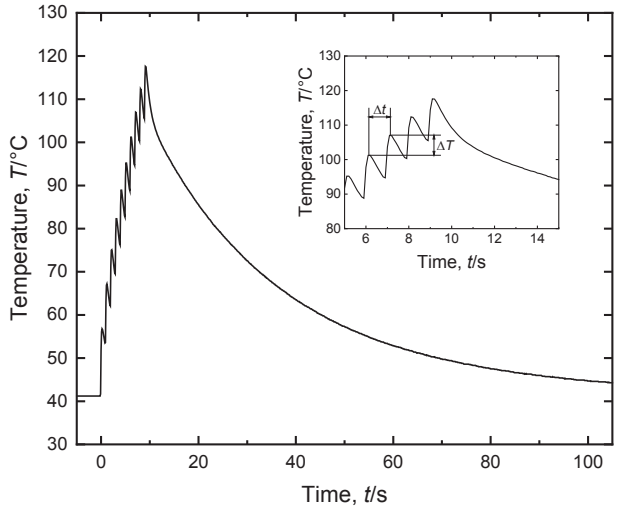

Fig. 2 Temperature variation of only the tray irradiated at 70 W laser power.

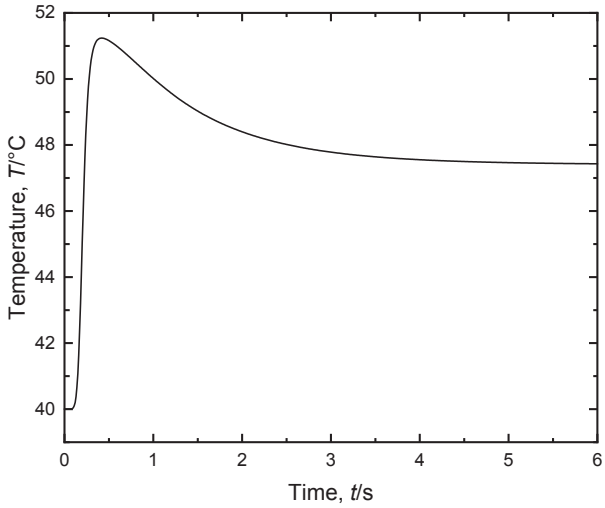

Fig. 4 Temperature variation at the center of the bottom surface in the numerical simulation with one movement of the heat source.

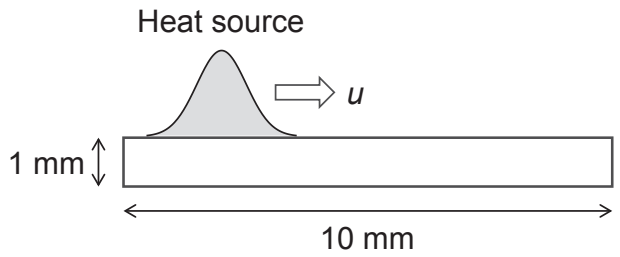

Fig. 3 Schematic of the numerical simulation model.

FEM calculation through commercially available software, Wolfram Mathematica. A 2D model was adopted by assuming uniformity in the hatch line direction due to the very high scan speed. For simplification, the simulation region was set to be a rectangle 10 mm wide and 1 mm high (Fig. 3). The initial temperature of the simulation was 40°C, and the boundary condition of the calculation region was no thermal loss. On the top surface of the region, the line heat source, whose intensity profile corresponded to the laser irradiation intensity, moved with speed u from left to right. The intensity profile of the line heat source $S(x, t)$ was set to be a Gaussian shape as follows:

$$S(x,t) = \alpha \frac{P}{D} \frac{N\tau_1}{\tau} \sqrt{\frac{2}{\pi r^2}} e^{-2\left(\frac{x-x_0-u(t-t_0)}{r}\right)^2}. \quad (4)$$

Here, α is laser absorptivity, P is laser power, and D is the depth of the specimen in the direction of the hatch line. N is the number of hatch lines, τ_1 is the time to scan one hatch line, τ is the time to finish scanning all of the hatch lines, and r is the laser spot radius. u is the mean moving speed in the perpendicular direction x to the hatch line during scanning of the hatch lines. x_0 and t_0 are the start position and the start time of scanning, respectively. In the numerical simulation, the laser power and the laser spot diameter were set to 70 W and 2.2 mm, respectively. The material for the numerical simulation was titanium alloy Ti–6Al–4V. The physical property values were held as constants, adopting the values specified in the fitting formula of the experimental data[7] at 40°C. The laser absorptivity was assumed to be 0.4.

Figure 4 shows the temperature history at the center of the bottom surface of the calculation region as the result of the numerical simulation for one complete scan of all of the hatch lines. The start time of scanning was set to be 0. The temperature rose as the heat source went through the center of the top surface. After that, the temperature fell, approaching a constant value over time the temperature distribution of the calculation region became uniform. The time to reach an almost uniform temperature distribution was about 3 s.

Considering the temperature history of the simulation, the change in the cooling curve gradient is thought to be caused by the uniformization of the temperature distribution in the specimen. Therefore, the initial part of the cooling process, which is influenced by the uniformization of the temperature distribution, was eliminated in the estimation of thermal loss from the cooling process. The thermal loss $L(T)$ was estimated from the temperature history from 3 s after the temperature was maximized.

The measured temperature history after 3 s in the cooling process was smoothed and differentiated to estimate the cooling rate in eq. (2). The estimated cooling rate dT/dt is plotted against temperature T with a fitting function in Fig. 5. The fitting function of the estimated cooling rate was used to estimate $L(T)$ while accounting for the temperature-dependent specific heat.

In addition, it is thought that the temperature measured early in the heating process was also influenced by the uniformization of temperature distribution. To estimate the influence of this uniformization on the measured temperature history, a 2D numerical simulation was performed. The simulation conditions remained consistent with those described above, except for the number of heat source movements: there were 10 movements at 1 s intervals. The simulation result is shown in Fig. 6. In spite the absence of thermal loss in the simulation, the step heights of the temperature history early in the process are higher than they are later. In the numerical simulation with one movement of the heat source, as shown in Fig. 4, it takes about 3 s for the temperature to be almost constant by uniformization of the temperature distribution. In the numerical simulation with 10 movements

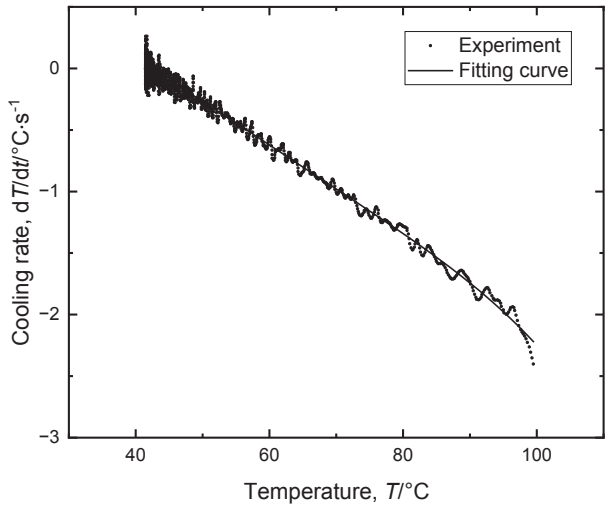

Fig. 5 Temperature dependence of cooling rate in the cooling process and its fitting curve.

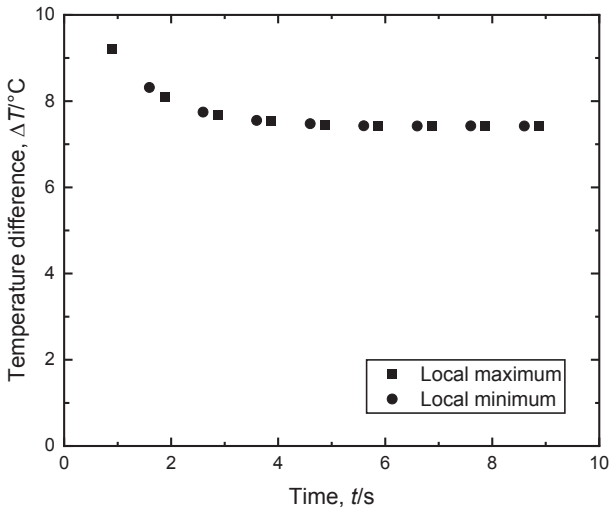

Fig. 7 Temperature difference of the adjacent temperature maximums and minimums in the heating process in Fig. 5.

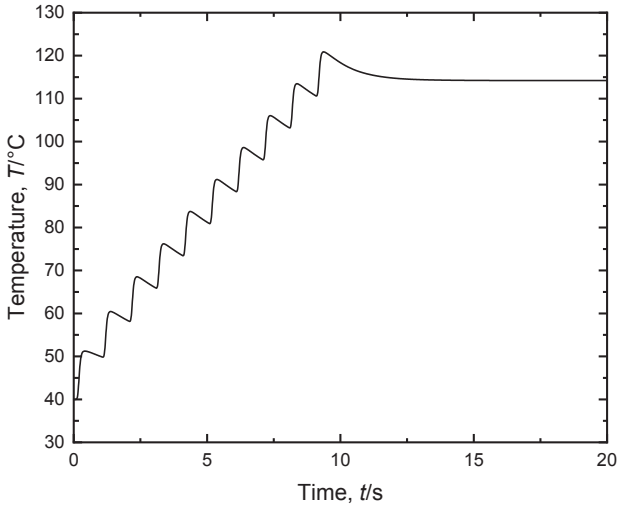

Fig. 6 Temperature variation at the center of the bottom surface in the numerical simulation with 10 movements of the heat source.

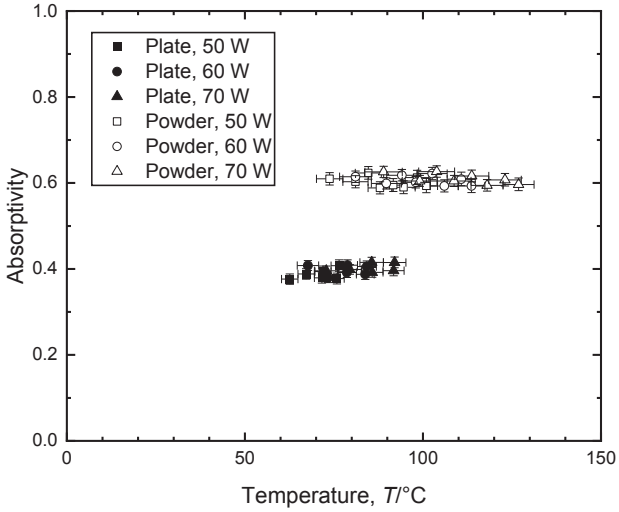

Fig. 8 Measured laser absorptivities of the tray and the powder.

of the heat source, it also seems that the higher temperature steps early in the process, i.e., about 3 s, are caused by the nonuniformity of temperature distribution. Of course, the temperatures measured after about 3 s are also influenced by the nonuniformity of temperature distribution. Nevertheless, the temperatures recorded approximately 3 s into the heating process encompass the impact of temperature distribution nonuniformity at the same level. Consequently, it is plausible that the effect on the temperature difference ΔT could be mitigated through cancellation.

To confirm the influence of the nonuniformity of the temperature distribution on the temperature difference ΔT, the temperature difference between adjacent maximums or minimums from in the numerical simulation shown in Fig. 6 are plotted in Fig. 7. The time of the plot is the intermediate value of times of the adjacent maximums or minimums. As seen from Fig. 7, the early temperature differences are larger than the latter differences, even with the same input energy. The temperature differences become almost constant after about 3 s. Therefore, laser absorptivity was calculated for the measured temperature history from about 3 s after the heating was started.

The measured laser absorptivity data are shown in Fig. 8. The laser absorptivity measured for the machined surface of the tray is labeled Plate. The laser absorptivity measured for the powder bedded in the tray is labeled Powder. The temperatures are intermediate values of temperatures of the adjacent maximums or minimums for ΔT calculation, and the range of error bars corresponds to the maximums or minimums. The temperatures used to calculate laser absorptivity are intermediate values of temperatures of the adjacent maximums or minimums for ΔT calculation, and the ranges of error bars of laser absorptivity are calculated from the temperatures of the adjacent maximums or minimums. The laser absorptivity of the powder was about 0.6, and that of the machined flat surface was about 0.4 for a normal incidence of laser light. The increase in laser absorptivity from the flat surface to the powder is likely attributable to the phenomenon of laser light undergoing multiple reflections within the powder. Although the measurement temperature range was narrow, no significant temperature dependence of laser absorptivity was seen.

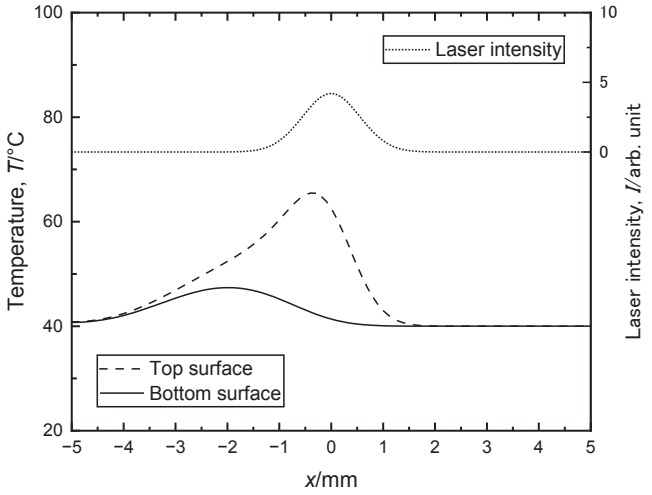

Fig. 9 Temperature distributions on the top and bottom surfaces and the laser intensity profile on the first movement of the laser from left to right in the numerical simulation.

In the experiments by Rubenchik *et al.*, the laser absorptivity of titanium alloy Ti–6Al–4V powder was about 0.7 for the laser wavelength of 970 nm,[5] and that for the flat surface of the same alloy was about 0.5 for the laser wavelength of 780 nm.[4] In the experiments using an integrating sphere by Brandau *et al.*, the absorptivity of titanium alloy Ti–6Al–4V powder was 0.7633 for the light wavelength of 1070 nm.[1] The laser absorptivity values measured in our experiments were slightly lower than those. However, the increase in laser absorptivity from the flat surface to powder was close to the ray-tracing simulation result by Boley *et al.*[8]

Due to the use of a thermocouple, which couldn't be positioned precisely at the laser irradiation site, there existed a disparity between the measured temperature and the actual temperature at the laser irradiation position. The measured temperature is thought to be less than the temperature at the laser irradiation position.

To check the influence of the measurement position, the temperature distribution was investigated by using the numerical simulation described above. The simulation conditions were the same as described above. Figure 9 shows the temperature distributions of the top and bottom surfaces and the laser intensity profile on the first movement of the laser from left to right. The temperature distribution on the top surface follows the laser intensity profile with almost the same shape immediately. On the other hand, the temperature distribution on the bottom surface experiences a delay due to the time taken for heat propagation from the top surface. The temperature on the top surface in the laser irradiation region is higher than that on the bottom surface and varies in the irradiation region, typically ranging a few tens of degrees Celsius higher. Therefore, the temperature of laser absorptivity shown in Fig. 8 is supposed to be a few tens of degrees Celsius lower than the laser irradiation area. To obtain more accurate results of the temperature dependence of laser absorptivity, it is necessary to reduce the uncertainty of temperature measurement.

In the actual additive manufacturing process, the temperature becomes above the melting point. However, the measured laser absorptivities were at the temperatures below 150°C. Expansion of the measurement temperature range to higher temperatures is needed in order to study laser absorption behavior at high temperatures as a future work.

4. Conclusion

To assess laser absorptivity in the context of laser powder-bed fusion additive manufacturing, we endeavored to measure laser absorptivity under conditions mirroring those of the actual manufacturing process. We achieved this by utilizing a commercially available additive manufacturing machine.

(1) We have succeeded in measuring the laser absorptivity of titanium alloy Ti–6Al–4V powder and the temperature dependence below 150°C by using a commercially available additive manufacturing machine under the same circumstances as in the manufacturing process.
(2) For titanium alloy Ti–6Al–4V powder used in additive manufacturing, the measured laser absorptivity was about 0.6 at a laser wavelength 1070 nm.
(3) For a machined surface of titanium alloy Ti–6Al–4V, the measured laser absorptivity was about 0.4 when exposed to laser light under normal incidence.

Acknowledgments

We would like to thank Mr. Masaru Suzuki for the experiments and Mr. Mitsugu Sato for preparation of the experimental devices.

REFERENCES

1) B. Brandau, A. Da Silva, C. Wilsnack, F. Brueckner and A.F.H. Kaplan: Mater. Des. **216** (2022) 110591.
2) T.J. Wieting and J.L. DeRosa: J. Appl. Phys. **50** (1979) 1071–1078.
3) M. Haag, H. Hügel, C.E. Albright and S. Ramasamy: J. Appl. Phys. **79** (1996) 3835–3841.
4) A.M. Rubenchik, S.S.Q. Wu, V.K. Kanz, M.M. LeBlanc, W.H. Lowdermilk, M.D. Rotter and J.R. Stanley: Opt. Eng. **53** (2014) 122506.
5) A. Rubenchik, S. Wu, S. Mitchell, I. Golosker, M. LeBlanc and N. Peterson: Appl. Opt. **54** (2015) 7230–7233.
6) J. Trapp, A.M. Rubenchik, G. Guss and M.J. Matthews: Appl. Mater. Today. **9** (2017) 341–349.
7) S. Sinha: J. Laser Appl. **31** (2019) 032008.
8) C.D. Boley, S.C. Mitchell, A.M. Rubenchik and S.S.Q. Wu: Appl. Opt. **55** (2016) 6496–6500.